

Short note

High-spin states in ^{160}Lu Lichang Yin¹, Yunzuo Liu^{1,2}, Jingbin Lu^{1,a}, Guangyi Zhao¹, Xianfeng Li¹, Xiaoguang Wu³, Guangsheng Li³, Shuxian Wen³, and Chunxiang Yang³¹ Department of Physics, Jilin University, Changchun 130023, PRC² Institute of Modern Physics, the Chinese Academy of Sciences, Lanzhou 730000, PRC³ China Institute of Atomic Energy, P.O. Box 275, Beijing 102413, PRC

Received: 21 May 2001 / Revised version: 13 July 2001

Communicated by D. Schwalm

Abstract. High-spin states of ^{160}Lu have been studied through the $^{144}\text{Sm}(^{19}\text{F}, 3n)$ reaction. The previously known $\pi h_{11/2} \otimes \nu i_{13/2}$ yrast band is extended from $I^\pi = 21^-$ to 25^- and a four quasiparticle band with configuration $\pi h_{11/2}[523]7/2^- \otimes \nu h_{9/2}[521]3/2^- \otimes (\nu i_{13/2})^2$ is reported.

PACS. 21.10.Re Collective levels – 23.20.Lv Gamma transitions and level energies – 27.70.+q $150 \leq A \leq 189$

The systematic features of signature inversion of the $\pi h_{11/2} \otimes \nu i_{13/2}$ band in the deformed odd-odd nuclei around $A = 160$ have been studied extensively in recent years [1–8], and it has been established that, with increasing spin, the level staggering changes from inverted to normal signature dependence, and the spin, at inversion point, decreases with increasing neutron number N in a chain of isotopes and increases with increasing proton number Z in a chain of isotones [2]. However, the existing data [9] shows that the variation pattern of the level staggering of the $\pi h_{11/2} \otimes \nu i_{13/2}$ band in ^{160}Lu is somewhat different from the general pattern described above. The inversion point has not been observed and the level staggering does not show the tendency towards the restoration of normal signature dependence at higher spins for the $\pi h_{11/2} \otimes \nu i_{13/2}$ band in ^{160}Lu . One of the motivations of the present study is to explore to what extent the variation behavior of the level staggering for the $\pi h_{11/2} \otimes \nu i_{13/2}$ band in ^{160}Lu is different from the general pattern of the level staggering for the $\pi h_{11/2} \otimes \nu i_{13/2}$ bands in the other odd-odd nuclei around $A = 160$ mass region.

The high-spin states of ^{160}Lu were populated through the $^{144}\text{Sm}(^{19}\text{F}, 3n)^{160}\text{Lu}$ fusion-evaporation reaction with 90 MeV ^{19}F ions provided by the HI-13 tandem accelerator at CIAE in Beijing. The ^{144}Sm target is the same as the one used in the previous work on ^{160}Lu [9]. The γ - γ coincidence events were recorded with an array of eleven Compton-suppressed HpGe detectors. A total of $\sim 80 \times 10^6$ two-fold events were recorded for the off-line

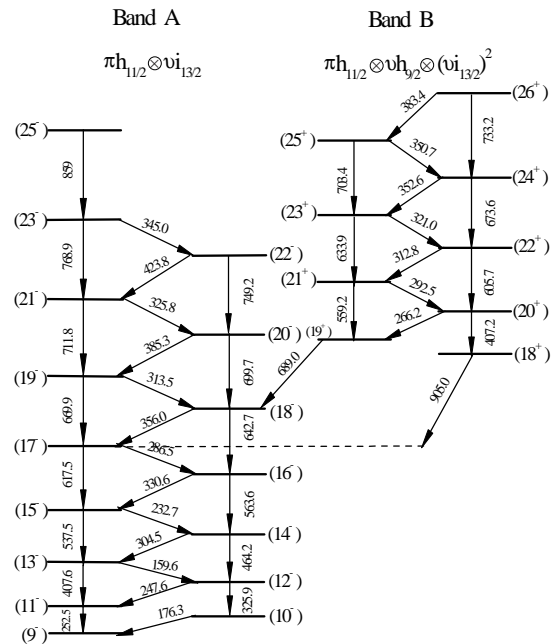


Fig. 1. Level scheme of ^{160}Lu proposed in the present work.

analysis. The DCO γ - γ matrix were created sorting on one axis the detectors lying at $\theta_1 = 38^\circ, 144^\circ$ and on the other those at $\theta_2 = 90^\circ$ with respect to the beam direction. With setting gates on stretched quadrupole transitions, the theoretical DCO ratios $I_{\gamma\text{gate}} = \theta_2(\theta_1)/I_{\gamma\text{gate}} = \theta_1(\theta_2)$ are ≈ 1 for stretched quadrupole transitions and ≈ 0.5 for

^a e-mail: jingbinlu@mail.jlu.edu.cn

Table 1. The experimental data obtained from the present work. The γ -ray intensities were normalized to the 247.6 keV transition ($12^- \rightarrow 11^-$), which is assumed to be 1000. In extracting the experimental $B(M1)/B(E2)$ ratios, the mixing ratio δ is assumed to be zero.

Band number	E_γ (keV)	$(I^\pi)_i \rightarrow (I^\pi)_f$	I_γ	Branching ratio	DCO ratio	$B(M1)/B(E2)$ (μ_N^2/e^2b^2)	
<i>A</i>	252.5	$(11^-) \rightarrow (9^-)$	975		0.96 (7)		
	325.9	$(12^-) \rightarrow (10^-)$	82	0.08 (1)	1.30 (47)	2.10 (0.25)	
	247.6	$(12^-) \rightarrow (11^-)$	1000		0.81 (4)		
	407.6	$(13^-) \rightarrow (11^-)$	500	0.91 (9)	1.25 (11)	2.12 (0.17)	
	159.6	$(13^-) \rightarrow (12^-)$	547		0.65 (5)		
	464.2	$(14^-) \rightarrow (12^-)$	210	0.27 (3)	0.94 (36)	1.97 (0.21)	
	304.5	$(14^-) \rightarrow (13^-)$	767		0.78 (5)		
	537.5	$(15^-) \rightarrow (13^-)$	639	1.2 (2)	1.21 (9)	2.05 (0.28)	
	232.7	$(15^-) \rightarrow (14^-)$	528		0.55 (4)		
	563.6	$(16^-) \rightarrow (14^-)$	287	0.48 (6)	1.36 (19)	2.28 (0.30)	
	330.6	$(16^-) \rightarrow (15^-)$	598		0.74 (5)		
	617.5	$(17^-) \rightarrow (15^-)$	542	1.2 (2)	1.06 (9)	2.31 (0.31)	
	286.5	$(17^-) \rightarrow (16^-)$	473		0.54 (5)		
	642.7	$(18^-) \rightarrow (16^-)$	371	1.1 (1)	1.12 (15)	1.58 (0.19)	
	356.0	$(18^-) \rightarrow (17^-)$	372		0.71 (6)		
	669.9	$(19^-) \rightarrow (17^-)$	370	1.6 (2)	1.16 (15)	1.97 (0.26)	
	313.5	$(19^-) \rightarrow (18^-)$	238		0.61 (6)		
	699.7	$(20^-) \rightarrow (18^-)$	240	0.87 (11)	1.39 (29)	2.35 (0.31)	
	385.3	$(20^-) \rightarrow (19^-)$	275		0.58 (7)		
	711.8	$(21^-) \rightarrow (19^-)$	196	1.5 (2)	1.04 (17)	2.39 (0.34)	
	325.8	$(21^-) \rightarrow (20^-)$	127		0.64 (8)		
	749.2	$(22^-) \rightarrow (20^-)$	106	0.83 (12)	1.20 (16)	2.60 (0.35)	
	423.8	$(22^-) \rightarrow (21^-)$	128		0.71 (12)		
	768.9	$(23^-) \rightarrow (21^-)$	142	1.5 (3)	1.20 (16)	2.98 (0.51)	
	345.0	$(23^-) \rightarrow (22^-)$	93		0.65 (15)		
859.0	$(25^-) \rightarrow (23^-)$	71		1.30(23)			
<i>B</i>	266.2	$(20^+) \rightarrow (19^+)$	280		0.63 (8)		
	559.2	$(21^+) \rightarrow (19^+)$	110	0.51 (10)	1.36 (29)	2.98 (0.60)	
	292.5	$(21^+) \rightarrow (20^+)$	216		0.46 (6)		
	605.7	$(22^+) \rightarrow (20^+)$	118	0.59 (14)	1.26 (27)	3.13 (0.76)	
	312.8	$(22^+) \rightarrow (21^+)$	200		0.47 (26)		
	633.9	$(23^+) \rightarrow (21^+)$	158	0.87 (27)	1.35 (31)	2.45 (0.78)	
	321.0	$(23^+) \rightarrow (22^+)$	182		0.55 (10)		
	673.6	$(24^+) \rightarrow (22^+)$	149	0.69 (21)	1.22 (23)	3.19 (0.96)	
	352.6	$(24^+) \rightarrow (23^+)$	216		0.54 (11)		
	703.4	$(25^+) \rightarrow (23^+)$	117	0.94 (19)	1.33 (32)	2.96 (1.24)	
	350.7	$(25^+) \rightarrow (24^+)$	125		0.67 (28)		
	733.2	$(26^+) \rightarrow (24^+)$	74	0.87 (26)	1.21 (45)	3.01 (0.90)	
	383.4	$(26^+) \rightarrow (25^+)$	85		0.65 (17)		
	Linking transitions	689.0	$(19^+) \rightarrow (18^-)$	173		0.64 (16)	
		904.0	$(18^+) \rightarrow (17^-)$	171		0.55 (12)	

pure dipole ones. The detectors were calibrated by using the ^{133}Ba and ^{152}Eu radioactive sources. The experimental results including transition energies, spin-parity assignments, γ -ray intensities, branching ratios, DCO ratios, and $B(M1)/B(E2)$ ratios are listed in table 1, grouped in sequences for band *A*, *B* and linking transitions.

Figure 1 is the level scheme proposed in the present work and the sample coincidence spectra supporting the level scheme are shown in fig. 2. The $\pi h_{11/2} \otimes \nu i_{13/2}$ yrast band (band *A*) reported in [9] has been extended from $I^\pi = 21^-$ to 25^- and band *B* is a new band proposed

in the present study. The spin and parity assignments of band *A* are adopted from [9]. Band *B* feeds band *A* via 689 and 905 keV transitions with DCO ratio of 0.64 and 0.55, respectively, indicating dipole character of both transitions. The competition of such energetic interband dipole transitions with the inband *E2* and *M1* transitions is indicative of *E1* multipolarity of these interband transitions and thus the parity of band *B* is assumed to be positive. Band *B* decays through transitions 324, 602, 568, 517, 494, and 481 keV as shown in fig. 2(d). These lines could not be placed unambiguously into the level scheme.

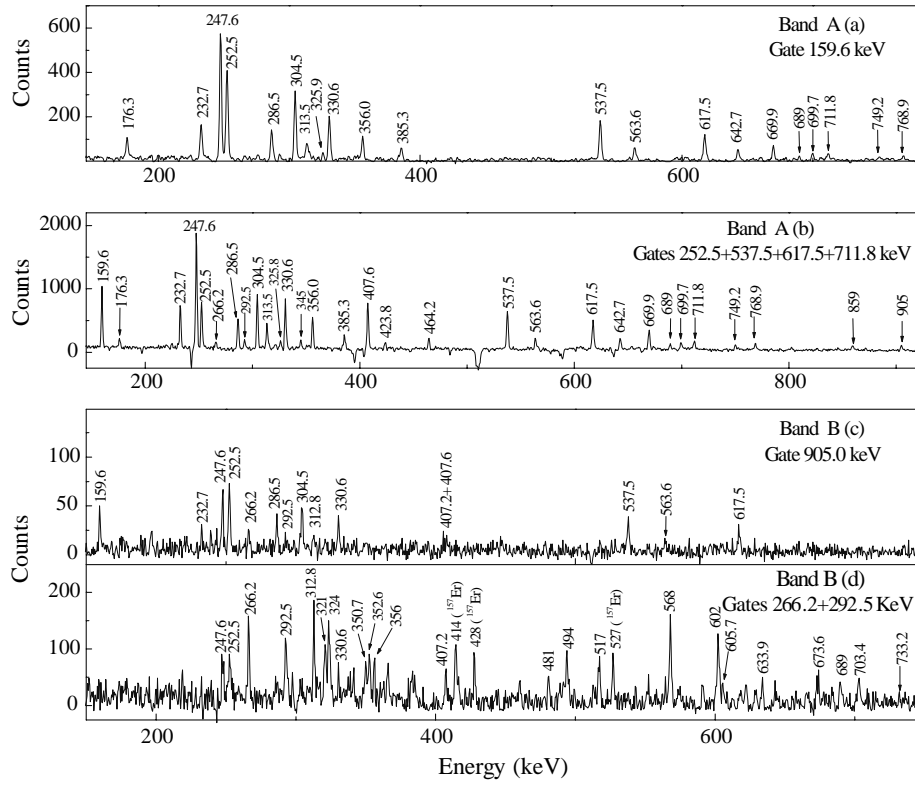


Fig. 2. γ - γ coincidence spectra of band A (a, b) and band B (c, d).

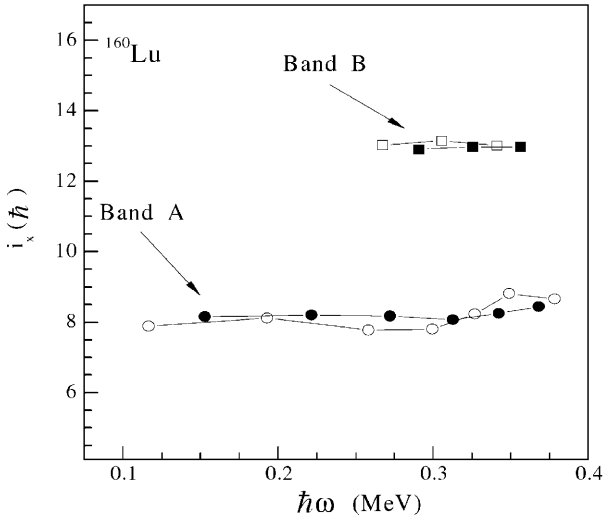


Fig. 3. Plots of alignment *versus* frequency for the two rotational bands assigned to ^{160}Lu . J_0 ($\text{MeV}^{-1}\hbar^2$) = 13.6 and J_1 ($\text{MeV}^{-3}\hbar^4$) = 154 for both band A and band B. The filled and open symbols refer to the even spin and odd spin, respectively.

The large alignment, as shown in fig. 3, and the high-excitation energy of band B suggest that band B is a four quasiparticle structure involving the coupling of the odd neutron and odd proton with a pair of aligned $i_{13/2}$ quasineutrons. Since the *BC* crossing occurs at $\hbar\omega \geq 0.35$ MeV in neighboring nuclei, the large alignment of band B is most likely contributed, in addition

to the alignments of odd neutron and odd proton, from the aligned $i_{13/2}$ quasineutron pair after *AB* crossing occurred in the unobserved initial part of band B. The *AB* crossing is not blocked and thus the odd neutron does not occupy the $i_{13/2}$ orbital in the four quasiparticle configuration of band B. $vi_{13/2}$ and $vh_{9/2}[521]3/2^-$ are the orbitals which are close to the neutron Fermi surface in ^{160}Lu and bands built on these orbitals have been the only bands reported in ^{159}Yb [10] and ^{161}Yb [11]. It is reasonable to assume that the odd neutron in the configuration of band B occupies the $vh_{9/2}[521]3/2^-$ orbital. $\pi h_{11/2}[514]9/2^-$, $\pi h_{11/2}[523]7/2^-$, $\pi g_{7/2}[404]7/2^+$, $\pi d_{3/2}[411]1/2^+$ and $\pi d_{5/2}[402]5/2^+$ are the orbitals close to the proton Fermi surface of ^{160}Lu . Due to the positive-parity assignment to band B and the neutron orbital assignment of $h_{9/2}[521]3/2^-$, only the orbitals with negative parity are the candidates of proton orbital in the configuration of band B. The experimental $B(M1)/B(E2)$ values are compared with those calculated for different possible configurations of band B using the geometric model of Donău and Frauendorf [12], as given in fig. 4. This comparison favors the configuration assignment $\pi h_{11/2}[523]7/2^- \otimes vh_{9/2}[521]3/2^- \otimes (vi_{13/2})^2$ to band B. The parameters used in the theoretical calculations are listed in table 2.

Figure 5 presents the level staggering for the $\pi h_{11/2} \otimes vi_{13/2}$ band in ^{160}Lu together with those of $^{162-168}\text{Lu}$ and $^{158-164}\text{Tm}$. The common feature of the odd-odd isotopes of $^{162-168}\text{Lu}$ and $^{160-164}\text{Tm}$ is that the level staggering has

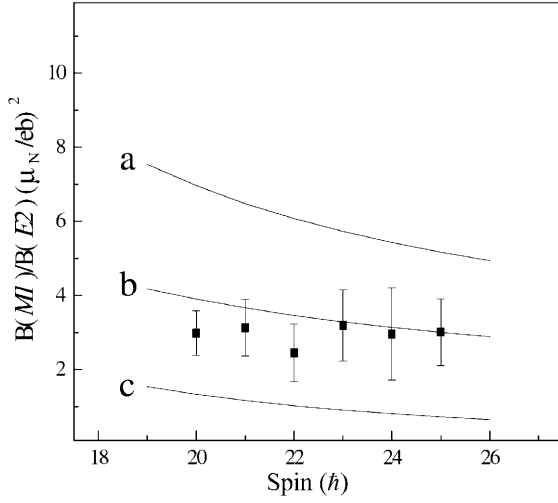


Fig. 4. Experimental $B(M1)/B(E2)$ ratios as a function of spin for band B in ^{160}Lu . The solid curves correspond to calculations based on geometric model. a) $\pi h_{11/2}[514]9/2^- \otimes \nu h_{9/2}[521]3/2^- \otimes (\nu i_{13/2})^2$; b) $\pi h_{11/2}[523]7/2^- \otimes \nu h_{9/2}[521]3/2^- \otimes (\nu i_{13/2})^2$; c) $\pi g_{7/2}[404]7/2^+ \otimes \nu h_{9/2}[521]3/2^- \otimes (\nu i_{13/2})^2$.

Table 2. Parameters used in the theoretical calculations of $B(M1)/B(E2)$ ratios.

Bands	$i_n(i_p)$ (\hbar)	$g_n(g_p)$	i_{nn} (\hbar)	Nuclei
$\pi h_{11/2}[514]9/2^-$	2.2	1.32		^{161}Lu [13]
$\pi h_{11/2}[523]7/2^-$	3.2	1.41		^{159}Lu [14]
$\pi g_{7/2}[404]7/2^+$	0.8	0.62		^{161}Lu [13]
$\nu h_{9/2}[521]3/2^-$	1.5	0.22	7.8	^{159}Er [15,16]
$g_R = 0.44$		$Q_0 = 4.37eb$		

inverted signature dependence and the magnitude of level staggering increases with decreasing neutron number at lower spins. However, the variation pattern of the level staggering with the spin for ^{160}Lu is quite different from those of the other odd-odd isotopes. For $^{162-168}\text{Lu}$ and $^{160-164}\text{Tm}$, with increasing spin, the two signatures cross each other at an inversion point and the level staggering changes from inverted signature dependence to normal signature dependence, and the spin at inversion point increases with decreasing N . For ^{160}Lu , with increasing spin, the two signatures do not come to cross each other and, after passing through a minimum, the magnitude of the signature inverted level staggering increases and it shows no sign of the restoration of normal signature dependence at higher spins as observed in the other odd-odd isotopes. It is worthwhile to note that such a saddle-shape behavior in ^{160}Lu is not consistent with the understanding that the dominance of Coriolis effect and thus the normal signature dependence should be restored at higher spins. Similar phenomenon can also be seen in the Thulium chain of isotopes, as shown in fig. 5, but the saddle-shape behavior in ^{158}Tm is less pronounced comparing to that of ^{160}Lu .

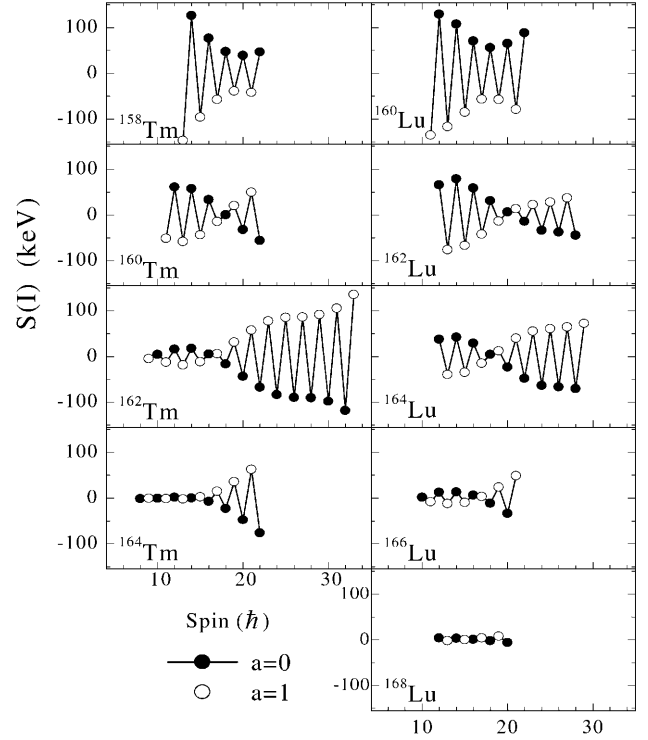


Fig. 5. Level staggering for the $\pi h_{11/2} \otimes \nu i_{13/2}$ band in ^{160}Lu (present work) compared to those in the $^{162-168}\text{Lu}$ and $^{158-164}\text{Tm}$ isotopes, $S(I) = E(I) - E(I-1) - [E(I+1) - E(I) + E(I-1) - E(I-2)]/2$. The filled symbols refer to the even spins ($\alpha = 0$) and the open symbols to odd spins ($\alpha = 1$). The even spins are expected to be favored. Data sources: ^{162}Lu [5,17,18], ^{164}Lu [5,19–21], ^{166}Lu [22–24], ^{168}Lu [25,26], ^{158}Tm [27,28], ^{160}Tm [29], ^{162}Tm [30], ^{164}Tm [31].

The authors are grateful to the HI-13 accelerator staff at CIAE for their help. This work was supported by the National Natural Science Foundation of China under the Grant No. 19975022 and by the Major State Basic Research Development Program under Contract No. G2000077400.

References

1. T. Komatsubara et al., Nucl. Phys. A **557**, 419c (1993).
2. Yunzuo Liu et al., Phys. Rev. C **52**, 2514 (1995).
3. S. Drissi et al., Nucl. Phys. A **604**, 63 (1996).
4. M.A. Cardona et al., Z. Phys. A **354**, 5 (1996).
5. M.A. Cardona et al., Phys. Rev. C **56**, 707 (1997).
6. L.L. Riedinger et al., Prog. Part. Nucl. Phys. **38**, 251 (1997).
7. Alpana Goel, A.V. Jain, Nucl. Phys. A **620**, 265 (1997).
8. Y.H. Zhang et al., High En. Phys. Nucl. Phys. **21**, 15 (1997).
9. H. Sun et al., Z. Phys. A **351**, 241 (1995).
10. T. Byrski et al., Nucl. Phys. A **474**, 193 (1987).
11. L.L. Riedinger et al., Nucl. Phys. A **347**, 141 (1980).
12. F. Donäü, S. Frauendorf, in *Proceedings of the Conference on High Angular Momentum Properties of Nuclei, Oak Ridge, Tennessee, 1982*, edited by N.R. Johnson (Harwood Academic, Chur, Switzerland, 1982) p. 143.
13. C.-H. Yu et al., Nucl. Phys. A **489**, 477 (1988).

14. Ma Yingjun *et al.*, *J. Phys. G* **21**, 937 (1995).
15. J. Simpson *et al.*, *J. Phys. G* **13**, 847 (1987).
16. J. Simpson *et al.*, *Eur. Phys. J. A* **1**, 267 (1998).
17. S.G. Zhou *et al.*, *J. Phys. G* **22**, 415 (1996).
18. S.L. Gupta *et al.*, *Phys. Rev. C* **56**, 1281 (1997).
19. X.-H. Wang *et al.*, *Nucl. Phys. A* **608**, 77 (1996).
20. P. Juneja *et al.*, *Phys. Rev. C* **53**, 1221 (1996).
21. S. Törmänen *et al.*, *Phys. Lett. B* **454**, 8 (1999).
22. D. Hojman *et al.*, *Phys. Rev. C* **54**, 90 (1992).
23. C.S.Lee *et al.*, *Eur. Phys. J. A* **8**, 1 (2000).
24. Guangyi Zhao *et al.*, *Eur. Phys. J. A* **9**, 299 (2000).
25. S.K. Katoch *et al.*, *Eur. Phys. J. A* **4**, 307 (1999).
26. J.H. Ha *et al.*, *Eur. Phys. J. A* **1**, 247 (1998).
27. M.A. Riley *et al.*, *Phys. Rev. C* **39**, 291 (1989).
28. S. André *et al.*, *Z. Phys. A* **332**, 233 (1989).
29. S. André *et al.*, *Z. Phys. A* **333**, 247 (1989).
30. J.M. Espino *et al.*, *Nucl. Phys. A* **640**, 163 (1998).
31. W. Reviol *et al.*, *Phys. Rev. C* **59** 1351 (1999).